

PV Optics: An Optical Modeling Tool for Solar Cell and Module Design

Preprint

B. Sopori, J. Madjdpour, Y. Zhang, and W. Chen

*To be presented at the Electrochemical Society
International Symposium
Seattle, Washington
May 2-6, 1999*



NREL

National Renewable Energy Laboratory

1617 Cole Boulevard
Golden, Colorado 80401-3393

NREL is a U.S. Department of Energy Laboratory
Operated by Midwest Research Institute • Battelle • Bechtel

Contract No. DE-AC36-99-GO10337

NOTICE

The submitted manuscript has been offered by an employee of the Midwest Research Institute (MRI), a contractor of the US Government under Contract No. DE-AC36-99GO10337. Accordingly, the US Government and MRI retain a nonexclusive royalty-free license to publish or reproduce the published form of this contribution, or allow others to do so, for US Government purposes.

This report was prepared as an account of work sponsored by an agency of the United States government. Neither the United States government nor any agency thereof, nor any of their employees, makes any warranty, express or implied, or assumes any legal liability or responsibility for the accuracy, completeness, or usefulness of any information, apparatus, product, or process disclosed, or represents that its use would not infringe privately owned rights. Reference herein to any specific commercial product, process, or service by trade name, trademark, manufacturer, or otherwise does not necessarily constitute or imply its endorsement, recommendation, or favoring by the United States government or any agency thereof. The views and opinions of authors expressed herein do not necessarily state or reflect those of the United States government or any agency thereof.

Available electronically at <http://www.doe.gov/bridge>

Available for a processing fee to U.S. Department of Energy
and its contractors, in paper, from:

U.S. Department of Energy
Office of Scientific and Technical Information
P.O. Box 62
Oak Ridge, TN 37831-0062
phone: 865.576.8401
fax: 865.576.5728
email: reports@adonis.osti.gov

Available for sale to the public, in paper, from:

U.S. Department of Commerce
National Technical Information Service
5285 Port Royal Road
Springfield, VA 22161
phone: 800.553.6847
fax: 703.605.6900
email: orders@ntis.fedworld.gov
online ordering: <http://www.ntis.gov/ordering.htm>



PV OPTICS: AN OPTICAL MODELING TOOL FOR SOLAR CELL AND MODULE DESIGN

Bhushan Sopori, Jamal Madjdpour, Yi Zhang, and Wei Chen
National Renewable Energy Laboratory
1617 Cole Boulevard
Golden, Co 80401

ABSTRACT

A brief description of the capabilities of *PV Optics*, a software package for the design and analysis of solar cells and modules, is given. Some specific applications of the software for the design of thick- and thin-film cells are given.

INTRODUCTION

Photovoltaic technology has advanced greatly in recent years – these advances have led to cost reduction of commercial PV energy, new materials and device designs for higher efficiency solar cells. Currently, solar cells and modules based on several different technologies are available in the marketplace. Crystalline silicon uses thicker wafers, while a-Si, CIGS, and CdTe are thin-film based cells. High-efficiency solar cell designs now include a number of features such as light-trapping, back-surface fields, textured and rough interfaces, reflective metallizations, and multijunction configurations. These features require design tools that can handle a variety of materials and cell configurations such as thick and thin cells, non-planar interfaces, and heavily-absorbing layers. Inclusion of these features undermines the usefulness of many software packages available for optical design. Here we briefly describe a new optical software package called *PV Optics* that includes these capabilities, and we discuss applications of the package for various high-efficiency cell designs.

BRIEF DESCRIPTION OF *PV OPTICS*

PV Optics is an easy-to-use software that accurately models the optics of most solar cells or modules, and provides information needed to design a device with maximum-effective light-trapping and optimum photocurrent. *PV Optics* can handle multilayer structures consisting of a combination of dielectrics, absorbing semiconductors, and highly-absorbing metallic layers with planar and nonplanar interfaces. Each of the layers may be “thin” or “thick” as compared to the coherence length of light in that layer. It uses this criterion to elect the application of the ray or wave optics to analyze the layer or the structure. This package outputs a variety of data in a form that can be easily used by a design engineer. These data include plots of the net reflectance, transmittance, and absorbance, AM1.5-weighted absorbed photon flux and its distribution within each layer, and the Maximum Achievable Current Density (MACD) from each active layer. MACD is the value of the photocurrent produced within an active layer corresponding to the generation of one electron-hole pair for each absorbed photon, and subsequent collection

of all of the generated carriers. In addition, it calculates and displays the current loss arising from optical absorption due to metallic contacts. A further description of the package is given elsewhere [1,2].

INPUT TO *PV OPTICS*

PV Optics starts with a typical module configuration, shown in Figure 1, which appears at the beginning of the operation. The module includes glass, encapsulation, AR coating, three semiconductor layers, a buffer, and a metal. One can modify this configuration and arrive at the desired device structure by simply deleting the unwanted regions by clicking on that region with a mouse. Figure 2 shows the resulting structure of an AR-coated and textured solar cell with a back metallization.

Selection of Device Configuration

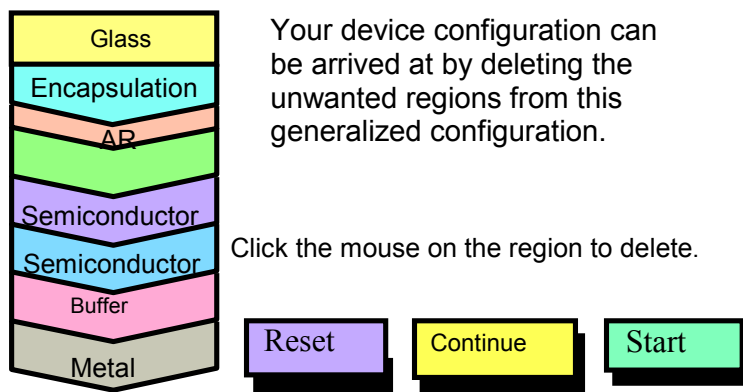


Figure 1. Illustration of PV Optics' "Selection of Device Configuration".

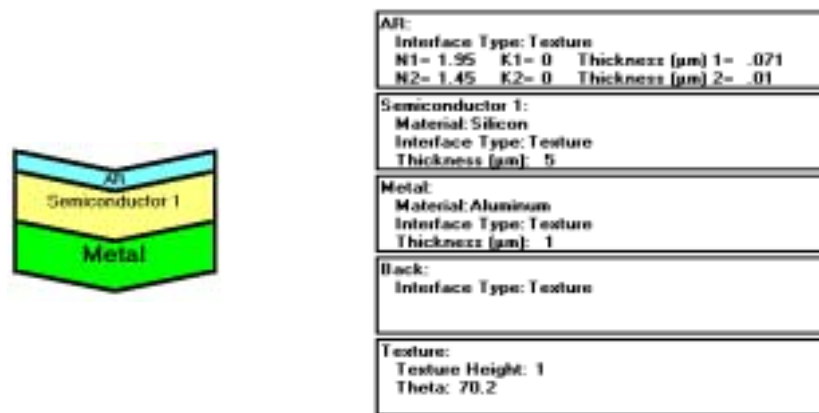


Figure 2. The configuration for a solar cell with front texture, AR coating, and a back metallized. The summary page on the right lists the input data.

PV Optics (Version 1) prompts the user to identify each interface type and input optical data for each layer that has wavelength-independent values. Each layer of the selected device structure appears as one page in the menu and provides the user with default values for the interface type (planar or textured), thickness (in μm), and the n and the k of each region. For example, the anti-reflection page provides the user with the default values for the interface type, and two-layer coating parameters— n_1 , k_1 , thickness1, and n_2 , k_2 , and thickness2. The default values correspond to standard materials and values used in the PV industry. The user can apply the default values or click on the area to change them. Likewise, the selection of each semiconductor page (up to three) provides the user with several choices of materials—"Silicon", "Amorphous-Silicon", "Amorphous-Silicon Top", "Amorphous-Silicon Middle", and "Amorphous-Silicon Bottom". Additional semiconductor data can be incorporated at request. Once all the input data is completed, the system provides a summary of the input data, as seen in Figure 2. Clicking on any specific compartment of the summary page opens up the corresponding page for corrections .

OUTPUT

The output of *PV Optics* is also oriented for a device engineer. Typically, the output is in the form of four plots consisting of (1) the reflectance, transmittance, and absorbance of the overall device, (2) absorbance of each active layer, (3) weighted (AM1.5) absorbance, and (4) distribution of absorbed photon flux. Furthermore, the plots are separated if the calculations use coherent mode. Here the plots are generated for: reflectance/transmittance (non-coherent), reflectance/transmittance (coherent), and weighted absorbance and photon flux.

RESULTS AND DISCUSSION

We present some applications of PV optics to the analysis and design of solar cells to show how *PV Optics* can handle thick and thin device configurations. Specifically, we will first examine how the optical properties and the photocurrent (J_{ph}) of a thick, crystalline-Si solar cell change on encapsulation into a module. Next, we will consider application to a-Si based cells.

Thick-cell and module design

For the first example, we consider analysis of a cell that is textured on both sides and has the following parameters: cell thickness 400 μm , texture height, $h = 4 \mu\text{m}$, texture angle = 70.2 $^\circ$. AR coating is a 2-layer coating consisting of 0.071 μm of Si_3N_4 (refractive index = 1.95) on 0.01 μm of SiO_2 ($n=1.45$). The cell has an Al back contact. Figure 3 shows the calculated parameters of the unencapsulated cell— its reflectance, absorbance in Si, and absorbance in the metal. This figure also includes the calculated MACD value of 41.37 mA/cm^2 . We see that reflectance has a broad null, and the metal absorption starts to become observable above a wavelength of 1 μm . Furthermore, the reflectance of the back-side is quite high and reaches about 70% at $\lambda=1.2 \mu\text{m}$. Figure 4 shows the weighted absorbance plot corresponding to the input spectrum of AM1.5, and includes the calculated value for the metal loss of 0.88 mA/cm^2 . It may be pointed out that because of the large thickness of the cell, this metal loss is quite low.

Figures 5 and 6 show the corresponding plots for the same cell after encapsulation. We see that the reflectance of the module does not exhibit a null, but has a minimum value of about 7%. The MACD is lowered, primarily because of the glass-reflectance, to 39.98 mA/cm², while the metal loss is reduced to 0.46 mA/cm².

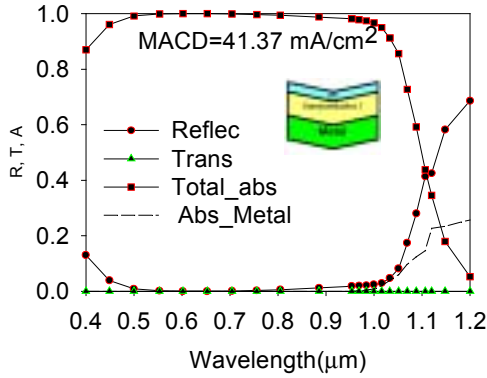


Figure 3. Calculated reflectance, transmittance, total semiconductor absorbance, and absorbance in the metal, for the unencapsulated cell structure shown in Figure 2.

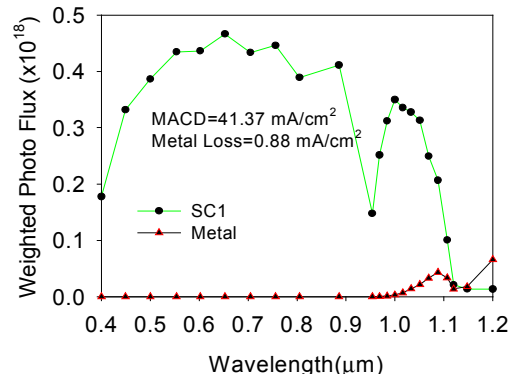


Figure 4. Calculated weighted absorbance of Si and Al, for the unencapsulated cell structure shown in Figure 2.

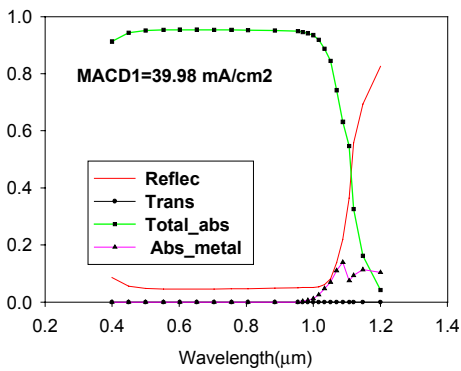


Figure 5. Calculated reflectance, transmittance, total semiconductor absorbance, and absorbance in the metal for the encapsulated cell.

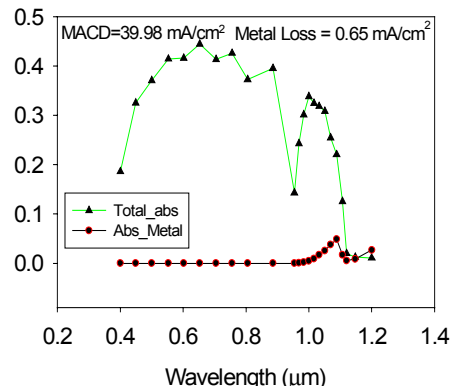


Figure 6. Calculate weighted absorbance in Si and in Al for the encapsulated cell.

Another important result generated by *PV Optics* is the distribution of the absorbed photon flux within the cell, for an AM1.5 incident spectrum. Such a distribution is needed to perform electronic design of the cell by modeling packages such as AMPS or PC1D. Figure 7 compares these distributions before and after encapsulation of the cell shown in Figure 2. Because the two distributions are very close to each other, the differences are not very clear on the scale shown in Figure 7. However, an inset is drawn in this figure that emphasizes the near-surface distribution. This inset shows that the maximum absorbance is higher for the unencapsulated cell, confirming its higher MACD value. It is useful to observe that the majority of absorption takes place in the first 100 μm of the cell.

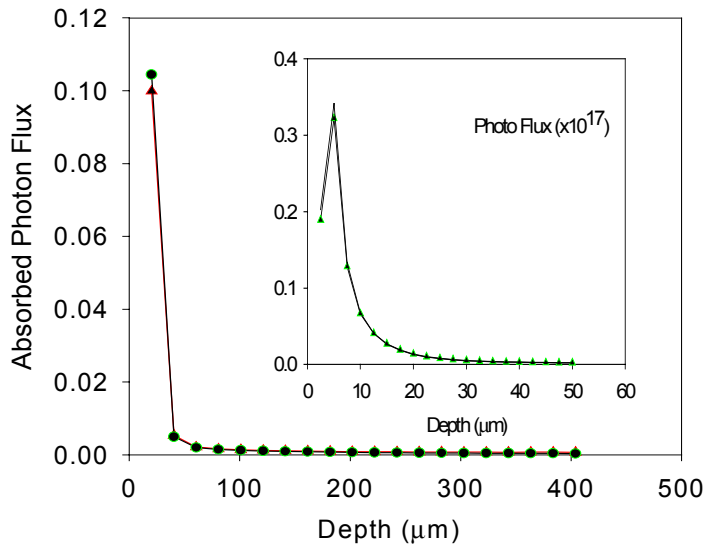


Figure 7. Absorbed photon flux as a function of depth before and after encapsulation. The inset is a magnified plot showing the near-surface profiles.

Applications to thin film a-Si solar cells

The current version of *PV Optics* handles devices having up to three junctions. The capabilities of the package are demonstrated here for an a-Si based cell, illustrated in Figure 8. This figure shows a three-junction cell with the materials that correspond to the following band gaps: $E_{g_top} = 1.8$ eV, $E_{g_middle} = 1.6$ eV, and the $E_{g_bottom} = 1.4$ eV. These are indicated as a-Si-T, a-Si-M, and a-Si-B, respectively. The cell has a V-shaped conformal texture in all layers with texture height and angle of $0.2 \mu\text{m}$ and 70° , respectively. The optical constants of the materials are already in the program. Here we assume thicknesses of the junctions as: $t_{Top} = 0.17 \mu\text{m}$, $t_{Mid} = 0.2 \mu\text{m}$, and $t_{Bot} = 0.2 \mu\text{m}$. These thicknesses are chosen only for demonstration purposes. The results of *PV Optics* are shown in Figures 9-11. Figure 9 shows the total reflectance, total absorbance of all semiconductor layers, and the absorbance in the metallic contact (which acts as the

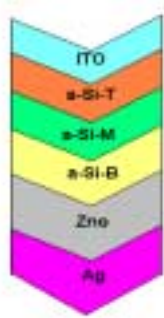


Figure 8. The structure of the three junction a-Si cell considered in the calculation.

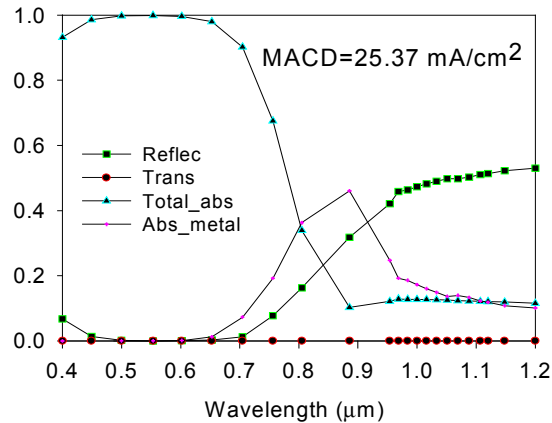


Figure 9. Calculated total reflectance, transmittance, and metal absorbance for the structure shown in Figure 8.

optical reflector), as a function of wavelength. Figure 10 shows the absorbance of each layer as a function of wavelength, for AM1.5 incident spectrum. This plot shows the MACD's of the top, middle, and the bottom layers to be 9.11 , 9.2 , and 8.07 mA/cm^2 ,

respectively. The current loss due to the metal is 6.42 mA/cm^2 . Figure 11 shows the distribution of the absorbed photon flux corresponding to AM1.5 illumination, as a function of depth. It should be pointed out that this depth profile shows an overlap of absorbance corresponding to the lateral overlap in Figure 8 of various cross sections along the cell thickness.

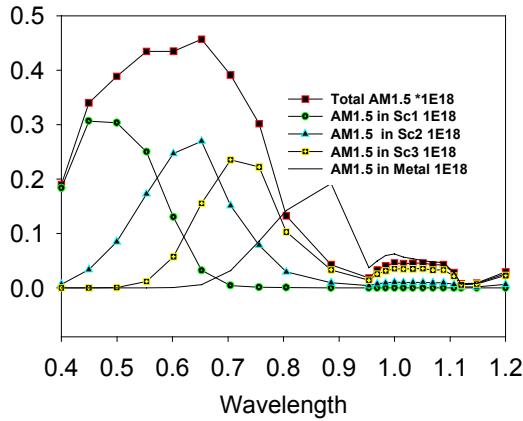


Figure 10. Absorbance spectra of the three-junction cell, and the weighted-metal absorbance.

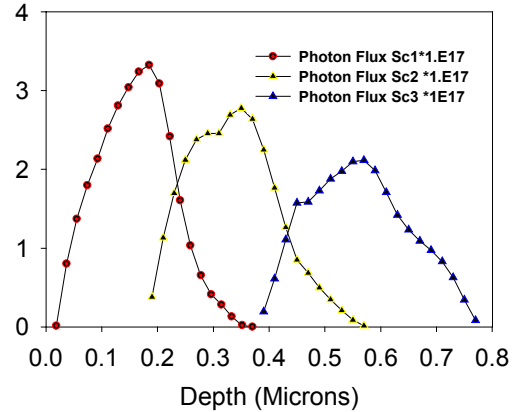


Figure 11. Distribution of the absorbed photon flux due to each cell.

As seen above, the thicknesses we have selected do not yield a current-matching condition; the current is limited by the bottom cell. It is clear that the bottom layer thickness must be increased to attain current matching. Figure 12 shows the effect of changing the thickness of the bottom layer in the structure of Figure 8. As expected, we see that as the film thickness is increased, the currents from the bottom cell increases; however, the currents of the other cells are also affected. We also see a general trend that the current in the top cell is only mildly affected. We studied in detail the effect of changing thicknesses of each cell to arrive at the current-matching condition. These

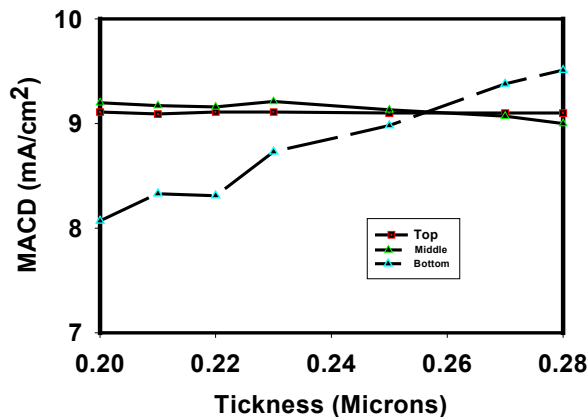


Figure 12. Dependence of the cell currents on the bottom cell thickness.

results (not included here) have shown that currents are most sensitive to the changes in the thickness of the middle cell. Furthermore, the effects are strongly controlled by the optics at the back surface. From Figure 12, the bottom cell thickness for the current-matching condition is about $0.255 \mu\text{m}$. It should be pointed out that the currents referred to here are the short-circuit currents, while the currents that need to be matched

correspond to the maximum power condition. But the design based on the short circuit currents is a good start that can be experimentally optimized.

Another feature of the PV Optics that we like to emphasize is its ability to include coherence effects for thin layers. "Version 1" includes recognition of completely coherent and completely incoherent structures and performs calculations accordingly. As an example, we consider a planar cell, 2 μm thick, with AR coating and a back Al contact. Figure 13 shows the calculated reflectance, transmittance, and absorbance plots with interference fringes arising from the coherence effects.

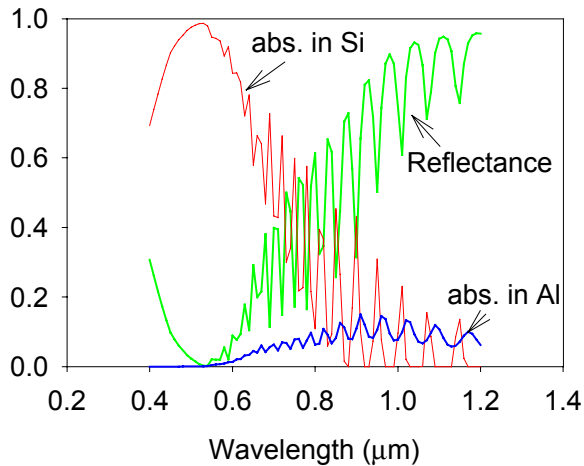


Figure 13. Reflectance, absorbance in the Si, and absorbance in Al for a 2- μm thin cell, showing the coherence effects.

CONCLUSION

We have briefly presented features of *PV Optics* that make it well suited for design and analysis of current solar cells and modules. The examples are given to illustrate applications for thick and thin cell design. *PV Optics* can also help gain insight into the mechanism of losses in photovoltaic devices, making it a useful design and teaching tool.

ACKNOWLEDGEMENT

This work was supported by US Department of Energy under Contract #DE-AC36-98-G010337 and by the DOE Center of Excellence for Advanced Materials Processing.

REFERENCES

1. B. L. Sopori, *Laser Focus*, **34**, 159 (Feb. 1998)
2. B. L. Sopori and T. Marshall, *Proc. 23rd IEEE Photovoltaic Specialists Conference*, 1993 (New York: IEEE).